# EDITORIAL BOARD




**Annual Subscription**

Pakistan: Rs 250 Foreign Countries: US$ 40 Overseas Air Mail Charges: US$ 10

**The Journal is published bi-annually**
**In April and October**

Sponsoring Agencies:
Ministry of Education, Government of Pakistan, Islamabad, Pakistan
Pakistan Science Foundation, Islamabad, Pakistan
Government College University, Lahore, Pakistan

Published by:
Riaz Ahmad for Government College University, Lahore, Pakistan

Printed at:
Mithas Enterprises Press , Lahore

# JOURNAL OF NATUTAL SCIENCES AND MATHEMATICS
# INFORMATION FOR AUTHORS

## 1. TYPES OF PAPER ACCEPTED

The Journal aims at publishing original research papers on Mathematics, Physics and Chemistry.

## 2. SUBMISSION OF MANUSCRIPTS

Manuscripts should be submitted in duplicate to the Section Editor concerned. All papers are refereed. The decision of the Editorial Board regarding the acceptance and publication of the paper will be final

## 3. PREPARATION OF MANUSCRIPT

### 3.1 Language and Style

All Submissions should be in English typed in double spacing on one side of the paper only with a Left hand margin of at least 4 cm. Mathematical expressions must be carefully printed, computer composed manuscripts on C.D. in Microsoft Windows/MS Word will be preferred for speedy publication.

### 3.2 Abstract

This should comprise a brief and factual summary of contents and should be suitable for direct use by abstracting journals. This will seldom require more than 200 words.

### 3.3 Section/Sub-Section Headings

Papers should be divided into sections / sub-sections and numbered as exemplified in the headings of this INFORMATION FOR AUTHORS.

### 3.4 References

References should be numbered consecutively in the text, e.g. "According to a recent theory [6]..." and collected at alphabetically at the end of the paper in following style.

6. I.M. Ghauri and P. Feltham, J. Nat. Sci. Math., 26, 63 (1986).

### 3.5 Illustrations

Line diagrams must be drawn in black ink on while paper; original and two copies are required. Photographs or half-tone reproduction should be in the form of highly glazed prints. A separate list of captions for illustrations should be provided

## 4. PROOFS

Only one set of proofs is sent to the authors for corrects

## 5. REPRINTS

A copy of the journal and twenty reprints are supplied free of cost. Additional reprints may be obtained on ordering in advance from the Managing Editor on payment.

PK ISSN 0022-2941; CODEN JNSMAC
Vol. 47, Nos. 1 & 2 (April & October 2007) PP-1-10

# PARAMETRIC INTERACTION IN A SINUSOIDAL PERIODIC PIEZOELECTRIC SEMICONDUCTOR STRUCTURE

**RASHID ALI* AND GHAZALA ANWAR****
*Department of Physics, University of the Punjab, Quaid-i-Azam Campus, Lahore-54590, Pakistan
** Department of Physics, Govt. College for Women, Baghbanpura, Lahore, Pakistan

**ABSTRACT:** In the present work, we have considered a sinusoidal modulated periodic piezoelectric semiconductor plasma as an alternative to the more often used Kronig-Penney model for investigating layered media. Further, we have investigated a three wave parametric interaction of a dipole electromagnetic pump wave, an extraordinary wave and coupled upper hybrid-acoustic and derived an expression for the threshold electric field necessary for the onset of the instability. Our results are presented graphically and a comparison is made with the case when the sinusoidal modulation is absent.

## 1. INTRODUCTION

In the present investigation we consider the parametric interaction of an electromagnetic pump wave, a coupled upper hybrid-acoustic wave and an extraordinary wave in a piezoelectric semiconductor which has a sinusoidal periodic structure. This parametric interaction has been investigated by Anwar et al. (1995) [1] for the case of a piezoelectric semiconductor plasma. However, we wish to extend this investigation to layered structures which have gained much technological importance in recent years. Super lattices or layered structures have been investigated for the past twenty years or so, beginning with the work of Baynham and Boardman (1968) [2] who studied the propagation of helicon waves in a Kronig-Penney type of periodic structure. Later, Narahari Achar (1987) [3] re-examined the same problem, but considered a sinusoidal modulated periodic structure instead of a Kronig-Penney type of model. Narahari Achar (1987) [3] choose the sinusoidal structure as an alternative to the Kronig-Penney model which has been used in many investigations of layered media [4-7].

## 2. ANALYTICAL TREATMENT

In the present work, we use Narahari Achar's (1987) [3] model of a periodic structure to consider the parametric interactions of the waves mentioned above. The unperturbed electron number density $n_o$, the lattice ion mass density $\rho$, the dielectric constant $\varepsilon$, the piezoelectric coupling constant $\beta$ and the elastic constant $C_e$ are all modulated in the following manner

$$a(x) = a_o\left[1 + \frac{\Delta a}{a_o}\cos(Qx)\right] \tag{1}$$

Where quantities with the subscript 'o' are average uniform and quantities like $\Delta a$ give the modulation amplitude of the quantity, and $2\pi/Q$ gives the period of modulation. Since we are

interested in three wave interactions, the phase matching conditions are expressed in the standard manner i.e.

$$\omega^P = \omega^T + \omega^S \quad ; \qquad k^P = k^T + k^S + \Delta k(x) \tag{2}$$

Here $\omega^P$, $\omega^T$ and $\omega^S$ are the frequencies associated with the pump wave, the scattered wave (extraordinary wave) and the slow wave (coupled upper hybrid-acoustic wave), respectively, and $k^P$, $k^T$ and $k^S$ are the corresponding wave numbers, and $\Delta k(x)$ is the wave number mismatch which occurs due to the inhomogeneity which results from the sinusoidal modulated periodic structure.

Our initial equations are the same as that in Anwar et al. (1995) [1] except that certain quantities (mentioned above) are modulated sinusoidally. For the case of completeness these quantities are given below:

$$\rho(x)\frac{\partial^2 u}{\partial t^2} - C_e(x)\frac{\partial^2 u}{\partial x^2} = -\beta(x)\frac{\partial E}{\partial x} \tag{3}$$

$$\frac{\partial E}{\partial x} = \frac{e}{\varepsilon(x)}n(x) - \frac{\beta(x)}{\varepsilon(x)}\frac{\partial^2 u}{\partial x^2} \tag{4}$$

$$\frac{\partial v}{\partial t} + (v.\nabla)v = -\frac{e}{m}[E + (v \times B)] - \nu v - v_T^2\frac{\nabla n}{n_{o(x)}} \tag{5}$$

$$\frac{\partial n}{\partial t} + \nabla.(nv) = 0 \tag{6}$$

$$\nabla \times \nabla \times E = \mu_o e\frac{\partial(nv)}{\partial t} - \mu_o\varepsilon(x)\frac{\partial E^2}{\partial t^2} \tag{7}$$

As in the above mentioned reference, the pump wave is assumed to be spatially uniform and $k^P$ is taken to be zero in the phase matching conditions given by equation (2). The first of equation (2) is same as that in Anwar et al. (1995) [1] but the second one differs in that, a $\Delta k(x)$ is added. This term is the wave number mismatch term and is there because of the periodic modulation of the medium which implies that certain quantities depend on the spatial coordinate '$x$'. We follow Anwar et al. (1995) [1] to derive an expression for the threshold electric field, necessary for the onset of instability i.e. we divide all physical quantities into components associated with fluctuations due to pump, the scattered extraordinary mode and the electrostatic fluctuations (coupled upper hybrid-acoustic mode).

$$n = n_o(x) + n^P + n^T + n^S$$

$$v = v^P + v^T + v^S$$
$$E = E^P + E^T + E^S \qquad (8)$$
$$B = B_o\hat{z} + B^T$$
$$u = u^S$$

We skip the algebraic details, which for most parts are the same as those in Anwar et al. (1995) [1] and give the expression for the threshold electric filed, below

$$E_{th}^P = |\{[A_1v^2 - (A_3 - A_4)v - A_5]/A_2\}|^{1/2} \qquad (9)$$

where

$$A_1 = \left\{[\alpha_r\omega^{P2} - \omega_{pe}^2(x)] \cdot \left\{\frac{2\omega_c^2}{\omega^{P3}}[\omega^{P2} - c^2k^{T2}(X)] + \frac{\omega_{pe}^2(x)}{\omega^P}\right\} + \left[\frac{2\omega_c^2}{\omega^P} + \frac{\omega_{pe}^2(x)}{\omega^P}\right]X_1 + \frac{4\omega_{pe}^2(x)\omega_c^2}{\omega^{P3}}\right\}$$
$$\cdot\{[2\omega^{S2} - k^{S2}v_T^2]X_2 - \omega_{pe}^2(x)[\rho(x)\omega^{S2} - C_e(x)k^{S2}]\}$$

$$A_2 = (e^2/m^2)k^Sk^T(x)\frac{\omega_{pe}^2(x)\omega^{P2}}{\omega^{P4} - 2\omega_c^2\omega^{P2} + \omega_c^4}X_2\left\{\left\{\alpha_r[(\omega^{P2} - c^2k^{T2}(x)] + \frac{\omega_{pe}^2(x)\omega_c^2}{\omega^{P2}} - \omega_{pe}^2(x)\right\}\right.$$
$$\left.\cdot\left\{\frac{\omega_c^2}{\omega^P}\left[1 + \frac{k^T(x)}{k^S}\right] - \omega^S\right\} - \left\{\alpha_r\omega^P\left[\alpha_r\omega_c^2 - \frac{\omega_c^4k^T(x)}{\omega^{P2}k^S} - \omega_c^2\right]\right\}\right\} \cdot e^{i\Delta k(x)x}$$

$$A_3 = \left\{[\alpha_r\omega^{P2} - \omega_{pe}^2] \cdot \left\{\frac{2\omega_c^2}{\omega^{P3}}[\omega^{P2} - c^2k^{T2}(x)] + \frac{\omega_{pe}^2(x)}{\omega^P}\right\} + \left[\frac{2\omega_c^2}{\omega^P} + \frac{\omega_{pe}^2(x)}{\omega^P}\right]X_1 + \frac{4\omega_{pe}^2(x)\omega_c^2}{\omega^{P3}}\right\}X_3$$

$$A_4 = \left[X_4 - \frac{4\omega_{pe}^4(x)\omega_c^2k^T(x)v_T^2}{\omega^{P2}(\alpha_r\omega^{P2} - k^{T2}(x)v_T^2)} \cdot \frac{1}{L}\right] \cdot \{[2\omega^{S2} - k^{S2}v_T^2]X_2 - \omega_{pe}^2(x)[\rho(x)\omega^{S2} - C_e(x)k^{S2}]\}$$

$$A_5 = [X_4 \cdot X_3]$$

In the above expressions for $A's$, $X_1$, $X_2, X_3, X_4$ and $\alpha_r$ are given below:

$$X_1 = \{\alpha_r[\omega^{P2} - c^2k^{T2}(x)] - \omega_{pe}^2(x)\}$$

$$X_2 = \left\{\rho(x)\omega^{S2} - C_e(x)k^{S2} - \beta^2(x)\frac{k^{S2}}{\varepsilon(x)}\right\}$$

$$X_3 = \left\{\omega^S\left[-(k^S v_T^2)\frac{1}{L}\right]\cdot\left[\rho(x)\omega^{S2} - C_e(x)k^{S2} - \beta^2(x)\frac{k^{S2}}{\varepsilon(x)}\right]\right\}$$

$$X_4 = \left[\alpha_r\omega^{P2} - \omega_{pe}^2(x)\right]\cdot\left\{-2\alpha_r c^2 k^T(x)\frac{1}{L_{KT}} - \frac{2\omega_{pe}^2(x)\omega_c^2 k^T(x)v_T^2}{\omega^P(\alpha_r\omega^{P2} - k^{T2}(x)v_T^2)}\frac{1}{L}\right\}$$

$$-\left\{\left[\frac{2\omega_{pe}^2(x)k^T(x)v_T^2}{(\alpha_r\omega^{P2} - k^{T2}(x)v_T^2)}\frac{1}{L}\right]\{\alpha_r[\omega^{P2} - c^2k^{T2}(x)] - \omega_{pe}^2(x)\}\right\}$$

$$\alpha_r = 1 - \frac{\omega_c^2}{(\omega^P - \omega^S)^2}$$

here

$$\omega_{pe}^2(x) = \omega_{po}^2\frac{[1 + (\Delta n/n_o)cos(Qx)]}{[1 + (\Delta\varepsilon/\varepsilon_o)cos(Qx)]}$$

$$\beta(x) = \beta_o[1 + (\Delta\beta/\beta_o)cos(Qx)]$$

$$\rho(x) = \rho_o[1 + (\Delta\rho/\rho_o)cos(Qx)]$$

$$\varepsilon(x) = \varepsilon_o[1 + (\Delta\varepsilon/\varepsilon_o)cos(Qx)]$$

$$k^T(x) = -k^S[1 + (\Delta k/k^S)cos(Qx)]$$

In the above, expressions $v_T$, $\omega_c$ and $\omega_{pe}$ are the electron thermal, gyrofrequencies and plasma frequencies, respectively, and

$$\frac{1}{L} = \frac{1}{n(x)}\cdot\frac{\partial n(x)}{\partial x} \quad ; \quad \frac{1}{L_{KT}} = \frac{1}{k^T(x)}\cdot\frac{\partial k^T(x)}{\partial x}$$

are the scale lengths of inhomogeneities due to the sinusoidal periodic modulation of the layered structure.

If we compare the above expressions with the threshold electric field expressions given in Anwar et al. (1995) [1], we see that if the periodic modulation of the piezoelectric semiconductor is absent, then $A_3, A_4$ and $A_5$ are equal to zero and the present expressions reduce to the case of Anwar et al. (1995) [1].

## 3. RESULTS AND DISCUSSIONS

Below we have numerically investigated for typical piezoelectric semiconductor values, the dependence of the threshold electric field $E_{th}$ on different parameters which enter into equation (10). Wherever possible we have compared these results to those of Anwar et al. (1995) [1]. In Figures (1a) and (1b) we have plotted $E_{th}$ against the background magnetic field $B_o$ for two different values of the background number density. Each Figure also shows the dependence of the threshold electric field at different points in the periodically modulated structure i.e. $Qx = 0, \frac{\pi}{4}, \frac{3\pi}{4}, \frac{5\pi}{4}, \frac{7\pi}{4}$. Figures (1a) and (1b) can be compared to the results of Figure (1) of Anwar et al. (1995) [1]. We see that for both number density cases the threshold value of the electric field is lower in the sinusoidal modulated periodic structure (present case) than in a simple piezoelectric semiconductor plasma (Anwar et al., 1995) [1] at $Qx = 0$. As $Qx$ increases, $E_{th}$ also increases and then decreases. Thus $E_{th}$ is also periodically modulated with sinusoidal variation of the medium.

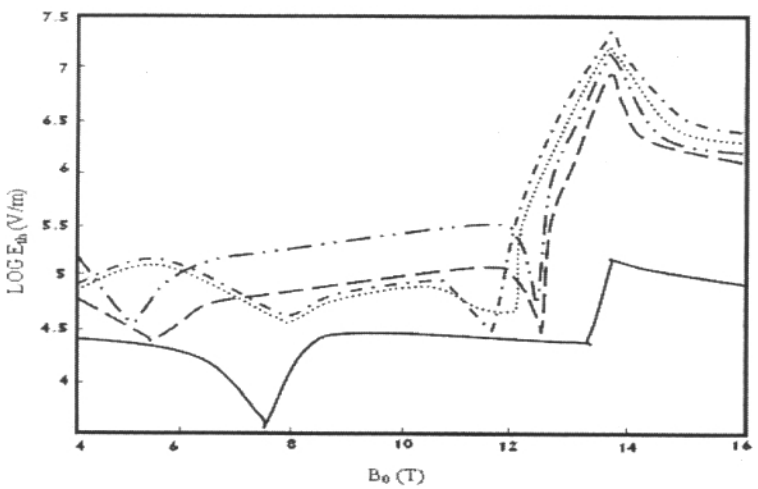


Fig. (1a). Threshold pump electric field $E_{th}(Vm^{-1})$ versus magnetic field $B_o(T)$ for $n_o = 7 \times 10^{28} m^{-3}$, $Q = 5 \times 10^5 m^{-1}$, $Qx = 0$ (_____), $\frac{\pi}{4}$ (.....), $\frac{3\pi}{4}$ (_ _ _), $\frac{5\pi}{4}$ (_ _ _), $\frac{7\pi}{4}$ (_ . _ .)

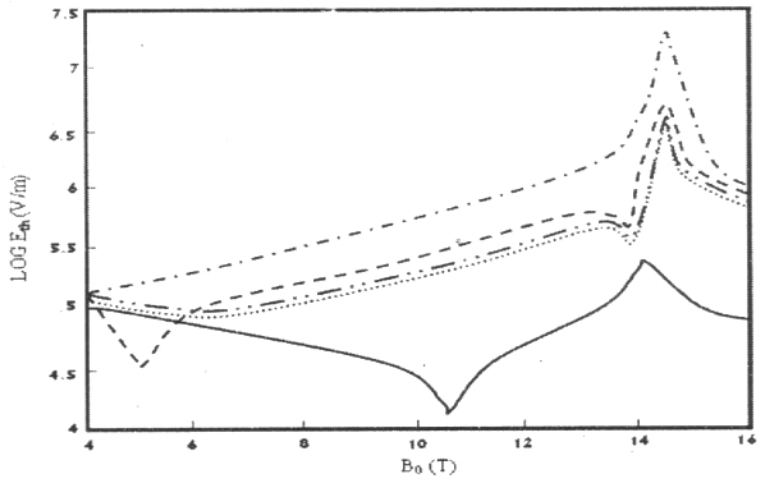


Fig. (1b). Threshold pump electric field $E_{th}(Vm^{-1})$ versus magnetic field $B_o(T)$ for $n_o = 2.44 \times 10^{24} m^{-3}$, $Q = 5 \times 10^5 m^{-1}$, $Qx = 0$ (——), $\frac{\pi}{4}$ (.....), $\frac{3\pi}{4}$ (— . . —), $\frac{5\pi}{4}$ (— — —), $\frac{7\pi}{4}$ (— . —)

Figures (2a) and (2b) show plots of the threshold electric field against the frequency $\omega^P$ (normalized by the electron plasma frequency) for two different values of the number density but at a fixed value of the background magnetic field ($B_o = 8T$ and $11.3T$). Comparison can be made with the Figure (2) of Anwar et al. (1995) [1] and we see that these results and the comparison are similar to those described in the preceding paragraph. In these Figures and in the plots of Figures (1) the value of all the modulational amplitudes is $\Delta a/a_o = 0.1$ .

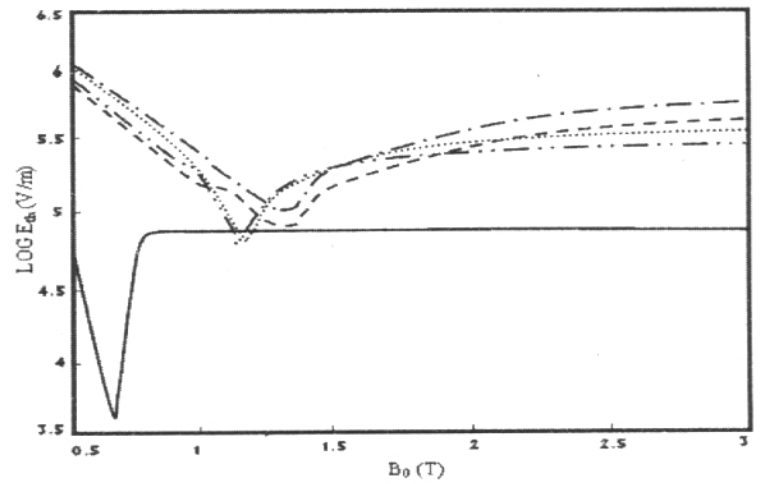


Fig. (2a). Threshold pump electric field $E_{th}(Vm^{-1})$ versus normalized pump frequency $\omega^P$ for $n_o = 2.44 \times 10^{24} m^{-3}$, $B_o = 8T$, $Q = 5 \times 10^5 m^{-1}$, $Qx = 0$ (——), $\frac{\pi}{4}$ (— . —), $\frac{3\pi}{4}$ (.....), $\frac{5\pi}{4}$ (— . . —), $\frac{7\pi}{4}$ (— —)

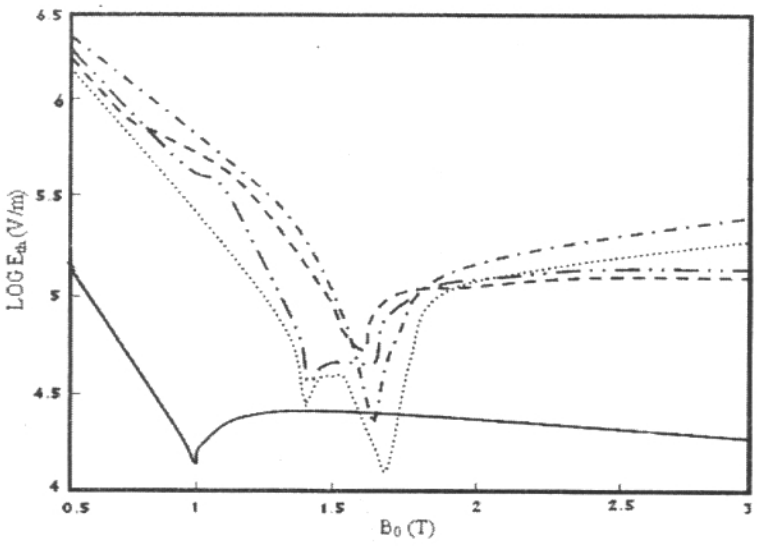


Fig. (2b). Threshold pump electric field $E_{th}(Vm^{-1})$ versus normalized pump frequency $\omega^P$for $n_o = 2.44 \times 10^{24}$, $B_o = 11.3T$, $Q = 5 \times 10^5 m^{-1}$,$Qx = 0$ (.....), $\frac{\pi}{4}$ (– . . –), $\frac{3\pi}{4}$ (———), $\frac{5\pi}{4}$ (- - - -), $\frac{7\pi}{4}$ (– · – ·)

Figures (3) and (4) show the variation of threshold electric field against $x$ (note that $Qx$ varies between 0 and 2π). Figure (3) is plotted for $n_o = 7 \times 10^{23} m^{-3}$ and the amplitude of modulation is taken as $\Delta n/n_o = 0.1$ and 0.4 in Figures (3a) and (3b), respectively. Whereas in figures (4) $n_o = 2.44 \times 10^{24} m^{-3}$. In both Figures (3) and (4) plots are made for two values of the background magnetic field ($B_o = 8T$ and $B_o = 11.3T$) and $\Delta n/n_o = 0.1, 0.4$, respectively. All the other modulational amplitudes are also taken as 0.4 when $\Delta n/n_o = 0.4$. We see that $E_{th}$ varies in a complicated fashion with increasing $x$, but a periodicity is maintained.

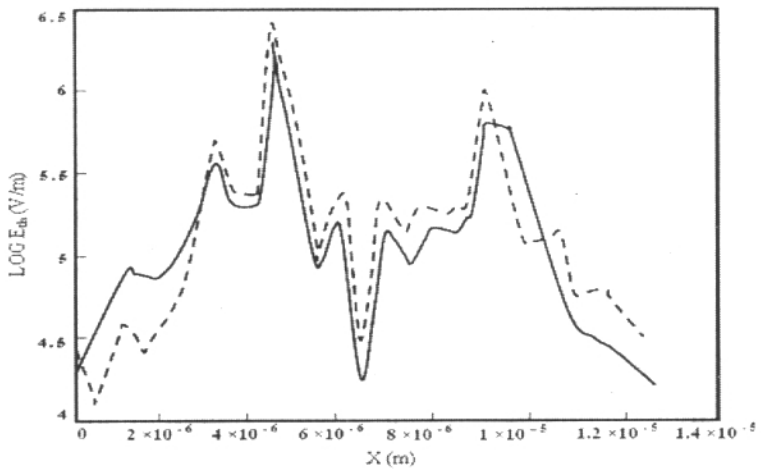


Fig. (3a). Threshold pump electric field $E_{th}(Vm^{-1})$ versus spatial distance $x(m)$ for $Qx = 0$ *to* $\pi$, $n_o = 7 \times 10^{29} m^{-3}$, $Q = 5 \times 10^5 m^{-1}$, $\Delta n/n_0 = 0.1$ and $B_o = 8T$(_____) , $B_o = 11.3T$ (_ _ _ _)

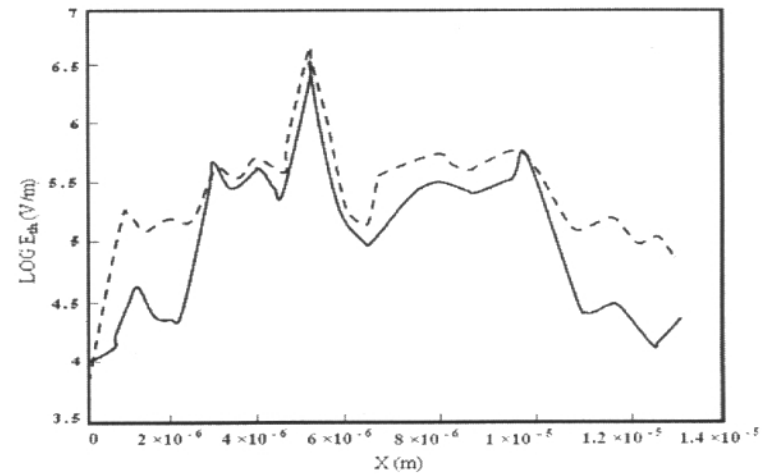


Fig. (3b). Threshold pump electric field $E_{th}(Vm^{-1})$ versus spatial distance $x(m)$ for $Qx = 0$ *to* $\pi$, $n_o = 7 \times 10^{29} m^{-3}$, $Q = 5 \times 10^5 m^{-1}$, $\Delta n/n_0 = 0.4$ and $B_o = 8T$( ) , $B_o = 11.3T$ ( )

We also note that for higher values of the magnetic field, the threshold values in general tend to be higher. As the amplitudes of modulation increases, the threshold value of the electric field also decreases (compare Figure 3a & 3b or Figure 4a & 4b). By comparing Figure 3 with 4, we see that as number density increases the threshold electric field also increases. Finally we note that all other numerical values pertaining to the different parameters entering into equation (10) are the same as those used in Anwar et al. (1995) [1].

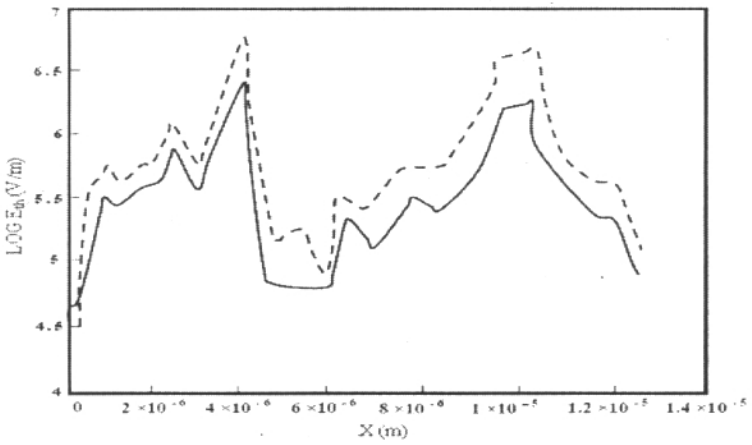


Fig. (4a). Threshold pump electric field $E_{th}(Vm^{-1})$ versus spatial distance $x(m)$ for $Qx = 0$ *to* $\pi$, $n_o = 2.44 \times 10^{24} m^{-3}$, $Q = 5 \times 10^5 m^{-1}$, $\Delta n/n_0 = 0.1$ and $B_o = 8T$( ) $B_o = 11.3T$ ( )

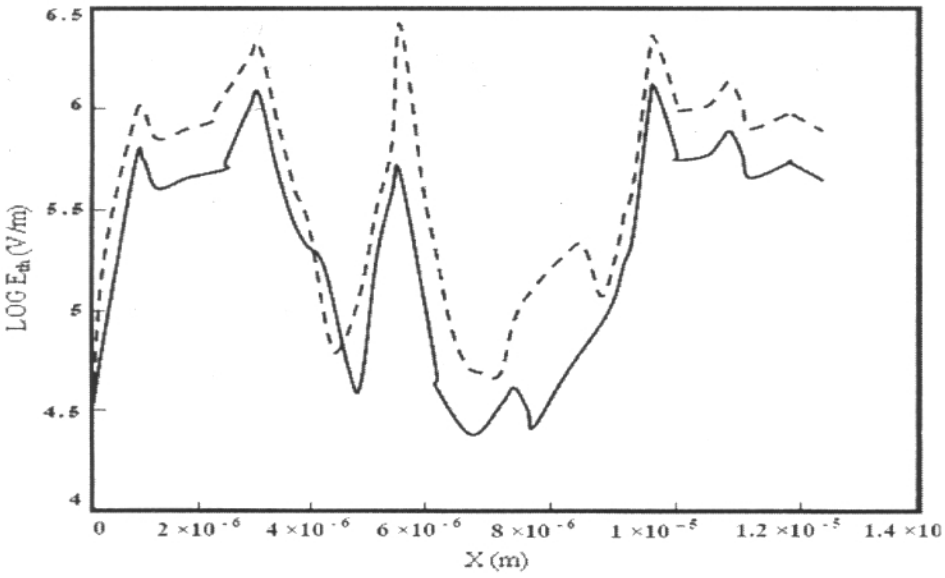


Fig. (4b). Threshold pump electric field $E_{th}(Vm^{-1})$ versus spatial distance $x(m)$ for $Qx = 0$ *to* $\pi$, $n_o = 2.44 \times 10^{24} m^{-3}$, $Q = 5 \times 10^5 m^{-1}$, $\Delta n/n_0 = 0.4$ and $B_o = 8T$( ) , $B_o = 11.3T$ ( )

## 4. CONCLUSION

In conclusion we note that we have investigated a parametric process in a layered medium, and have used the model developed by Narahari Achar (1987) [2] to approximate or replace the Kronig-Penney model by a sinusoidal modulated periodic structure. The parametric interaction

that we have considered here is the same as that was considered by Anwar et al. (1995) [1] for an ordinary piezoelectric semiconductor plasma. We observe that the periodicity of the structure affects the behavior of the threshold electric field necessary for the onset of parametric instability. The threshold values in general tend to differ from the case when there is no modulation and have a variation which depends on the sinusoidal periodic modulation of the layered piezoelectric semiconductor plasma. We note here that the introduction of a sinusoidal modulated periodic structure is similar to including an inhomogeneity in the model. However, the difference is that most inhomogeneous plasmas tend to have monotonic gradients in the number densities etc. but in the model that we have used the sinusoidal periodic modulation introduces inhomogeneities in the different physical quantities and the gradients associated with these periodically change magnitudes as well as signs.

## REFERENCES

1. G. Anwar., H. Saleem and H. A. Shah, J. Phys.:Condens. Matter, **7**, 45 (1995).
2. A. C. Baynham and A. D. Boardman, J. Phys. A 1, 363 (1968)
3. B. N. Narahari Achar, Phys. Stat. Sol. b, 143, 235 (1987).
4. J. C. Mann, M. Altarelli, H. Sigg, P. Wyder, L. L. Chang and L. Esaki, Surface Sci., **113**, 347 (1982).
5. S. Das Sarma and J. J. Quinn, Phys. Rev. B, **25**, 7603 (1982).
6. A. Tselis, G. Gonzaliz De La Cruz and J. J. Quinn, Solid State Commun., **47**, 43 (1983).
7. A. Tselis and J. J. Quinn, Phys. Rev. B., **29**, 2021 (1984).

PK ISSN 0022-2941; CODEN JNSMAC
Vol. 47, Nos. 1 & 2 (April & October 2007) PP-11-23

# MAGNETOSTATIC SURFACE WAVES IN A LAYERED (DIELECTRIC/MAGNETIC/CONDUCTOR) WAVEGUIDE STRUCTURE

**BURHAN ZAMIR AND RASHID ALI**
Department of Physics, Quaid-i-Azam Campus, University of the Punjab, Lahore-54590, Pakistan

**ABSTARCT:** The dispersion of magnetostatic surface waves propagating in a composite (layered) waveguide structure of a linear dielectric, ferrite film and a conducting medium have been studied. We have numerically investigated the dependence of effective wave index on the propagation frequency. Limiting cases with poor and with infinite conductivity have also been discussed. It is found that for the case of poor conductivity, our dispersion relation reduces to the well known expression of Damon-Eshbach surface wave mode for tangentially magnetized ferrite film, and in the other case we solve the dispersion relation in order to determine the effects of infinite conductivity on the dispersion characteristics.

## 1. INTRODUCTION

The magnetostatic surface waves (MSSWs), as the name implies, propagate along a surface. The externally applied magnetic field is parallel to the surface and the direction of propagation is perpendicular to this field, or at some angle to it. Usually these waves are discussed for thin magnetic films for which two coupled surfaces are involved [1]. We know that semiconductor physics and magnetism are established subfields of condensed matter physics that continue to reveal a rich variety of new phenomena, often in new types of solid state materials including layered and composite media etc. In the layered media, interactions of electromagnetic, magnetostatic and spin waves with carriers can be studied using adjacent magnetic, semiconductor and dielectric layers. The realization of surface waves in composite structures consisting of two or three materials has been a dream of material physicist. For example, dispersion relation of nonlinear electromagnetic surface waves in a structure consisting of a dielectric film, bounded by a nonlinear dielectric cover and a gyromagnetic ferrite substrate has been investigated by Shabat and Pelzl [2]. Dispersion relations of the transverse electric (TE) waves at an interface between linear gyromagnetic and nonlinear dielectric media have been investigated by Boardman et al. [3]. Transverse magnetic (TM) surface waves in a three layered antiferromagnet/superconductor/linear dielectric structure have been examined by Hamada et al. [4]. In another paper, Hamada et al. [5] investigated the transverse magnetic (TM) surface waves in a similar antiferromagnet/semiconductor/superconductor waveguide structure. Magnetostatic surface waves (MSSWs) have also been examined by various authors. For example, the dispersion relation of magnetostatic surface waves propagating in a ferromagnetic

film of finite dimensions has been studied by O'Keeffe and Patterson [6]. MSSWs using adjacent layers of "ferrite/superconductor" and "nonlinear dielectric/ferrite/left-handed material" have been investigated by Semenov et al. [7] and Hamada et al. [8], respectively.

## 2. GEOMETRY OF THE PROBLEM AND DISPERSION RELATION

In the present work, we investigate the propagation of magnetostatic surface waves (MSSWs) propagating in a composite structure consisting of a linear dielectric, ferrite (YIG) film and a conducting material. These types of layered structure may be used as a waveguide for microwave applications. The geometry of composite structure for the propagation of magnetostatic surface waves to be analyzed is shown in Figure 1.

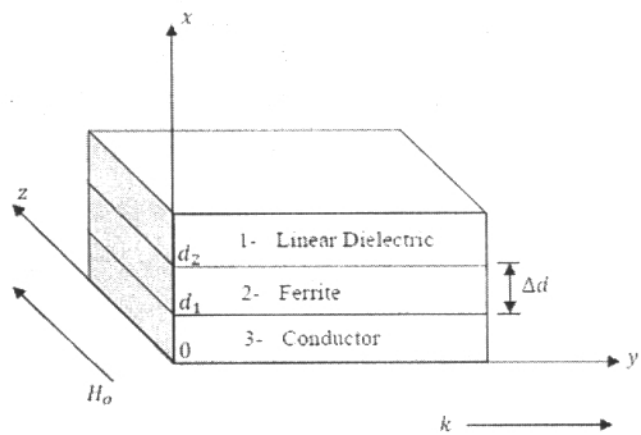


**Figure 1.** Composite structure of linear dielectric, Ferrite (YIG) and a conducting material for the propagation of magnetostatic surface waves.

We consider a ferrite film of YIG $(d_1 \leq x \leq d_2)$ adjacent to the semi-infinite thick layers of linear dielectric $(x > d_2)$ and a conducting material$(x < d_1)$. In this configuration, each of these materials extends to infinity in the yz-plane. A uniform magnetic field $H_0$ is applied in +z direction. For simplicity, we consider the propagation of these surface waves in the +y direction and that all the components of the fields are taken to be proportional to $e^{i(\omega t - ky)}$ which are

independent of z, where $k$ is the wave vector in the +y direction and $\omega$ is the wave frequency. With this geometry, a magnetostatic surface wave can be propagated in our proposed structure. In the coordinate system adopted, the condition $\partial/\partial z = 0$ is valid for magnetostatic surface waves (MSSWs), which means field does not vary in the z-direction [8]. A solution can be obtained in the form of transverse electric TE$(E_z, H_x, H_y)$ mode [7]. Transverse electric (TE) waves do not have a component of the electric field in the direction of propagation $(i.e. E_y = 0)$. In the present analysis, we consider transverse electric wave mode inherent to a ferrite, since we are interested only in the magnetostatic surface waves.

Since all the field components are taken to be proportional to $e^{i(\omega t - ky)}$, thus for TE mode of magnetostatic surface wave, we take the solutions of Maxwell's equations in the form of electric and magnetic field vectors as given below:

$$H = (H_x, H_y, 0)e^{i(\omega t - ky)} \quad (1)$$

$$E = (0, 0, E_z)e^{i(\omega t - ky)} \quad (2)$$

**Calculations for linear dielectric $(x > d_2)$**

By replacing the time derivatives by $i\omega$, the relevant Maxwell field equations for the linear dielectric medium are given by

$$\nabla \times H_1 = i\omega\varepsilon_0\varepsilon_l E_1 \quad (3)$$

$$\nabla \times E_1 = -i\omega\mu_0 H_1 \quad (4)$$

'1' refers to field vectors corresponding to the linear dielectric medium (as shown in Figure 1), whereas $\varepsilon_o$, $\mu_o$ are the permittivity and permeability of the free space and $\varepsilon_l = \varepsilon_1/\varepsilon_o$ is the dielectric constant of the linear medium with permittivity $\varepsilon_1$, respectively. Taking curl of equation (4) and using (3), we have

$$\nabla(\nabla \cdot E_1) - \nabla^2 E_1 = \omega^2 \varepsilon_o \mu_0 \varepsilon_l E_1$$

Since for a linear dielectric medium $(\nabla \cdot E_1 = 0)$, above equation reduces to

$$\nabla^2 E_1 = -k_0^2 \varepsilon_l E_1 \tag{5}$$

where $k_0^2 = \frac{\omega^2}{c^2}$, wave vector of free space. Now we solve the left hand side of equation (5)

$$\nabla^2 E_1 = \left(\frac{\partial^2}{\partial x^2} + \frac{\partial^2}{\partial y^2} + \frac{\partial^2}{\partial z^2}\right)(0\,, 0, E_{z1}) e^{i(\omega t - ky)} = \frac{\partial^2}{\partial x^2} E_{z1} e^{i(\omega t - ky)} - k^2 E_{z1} e^{i(\omega t - ky)} +$$

0

The third term is zero, because we assume our composite structure to be infinite in extent in the z-direction, which is tantamount to assuming that electric field does not vary in the z-direction and that edge effects are negligible. Since $E_{z1}$ is the only component of the electric field vector, therefore, it is convenient to take $E_{z1}$ instead of using $E_1$ in the subsequent calculations. Using above expression in equation (5), we get

$$\frac{\partial^2 E_{z1}}{\partial x^2} = (k^2 - k_0^2 \varepsilon_l) E_{z1}$$

For a semi-infinite thick layer of linear dielectric $(i.e.\ x \to +\infty)$, a simple solution of above equation for $(x > d_2)$ is given by

$$E_{z1} = A e^{-k_1 x} \tag{6}$$

where $k_1 = \sqrt{k^2 - k_0^2 \varepsilon_l} = \sqrt{k_0^2 (n^2 - \varepsilon_l)}$, and $n = k/k_o = ck/\omega$ is the effective wave index. From the Maxwell's equation (4) and using above relation for $E_{z1}$, the magnetic field components for the linear dielectric are given by

$$H_{x1} = \frac{k}{\omega \mu_o} A e^{-k_1 x} \tag{7}$$

$$H_{y1} = \frac{i k_1}{\omega \mu_o} A e^{-k_1 x} \tag{8}$$

**Calculations for a conductor $(x < d_1)$**

The relevant Maxwell field equations for a conducting medium are given by

$$\nabla \times H_3 = (\sigma + i\omega\varepsilon_0\varepsilon_c)E_3 \tag{9}$$

$$\nabla \times E_3 = -i\omega\mu_0 H_3 \tag{10}$$

'3' refers to field vectors corresponding to the conducting medium, whereas $\varepsilon_c = \varepsilon_3/\varepsilon_o$ and $\sigma$ are the dielectric constant of the conducting medium with permittivity $\varepsilon_3$ and the conductivity respectively. Using the similar procedure as done for the calculations of linear dielectric, we get the following differential equation:

$$\frac{\partial^2 E_{z3}}{\partial x^2} - k_3^2 E_{z3} = 0$$

where $k_3 = \sqrt{k_0^2\left(\frac{i\sigma\omega\mu_o}{k_o^2} + n^2 - \varepsilon_c\right)}$,

For a semi-infinite thick layer of conducting medium $(i.e.\ x \to -\infty)$, a solution of above differential equation for $(x < d_1)$ is $E_{z3} = Be^{k_3 x}$ (11)

From equation (10) and using above relation for $E_{z3}$, the magnetic field components for the conducting medium are

$$H_{x3} = \frac{k}{\omega\mu_o} Be^{k_3 x} \tag{12}$$

$$H_{y3} = \frac{-ik_3}{\omega\mu_o} Be^{k_3 x} \tag{13}$$

**Calculations for ferrite (YIG) film $(d_1 \le x \le d_2)$**

To find out the equations comprising the magnetostatic approximation to Maxwell's equations, we follow the procedure given in Stancil [9]. Maxwell Field equations for a magnetic medium (i.e. YIG) can be written as

$$\nabla \times H_2 = \varepsilon_2 \frac{\partial E_2}{\partial t} \tag{14}$$

$$\nabla \times E_2 = -\mu_o \frac{\partial}{\partial t}(H_2 + M_2) \tag{15}$$

where '2' refers to field vectors corresponding to the ferrite and $\varepsilon_2$ is the permittivity of the magnetic medium. In the 2nd equation we have used the value of magnetic field given by, $B_2 = \mu_0(H_2 + M_2)$, where $M_2$ is the magnetization. Taking cross product of equation (14) and using (15), we have

$$k(k \cdot H_2) - k^2 H_2 = -\omega^2 \varepsilon_2 \mu_0 (H_2 + M_2)$$

$\nabla \cdot B_2 = 0$ gives us $k \cdot H_2 = -k \cdot M_2$ , using this fact in above equation and after some simplification we get

$$H_2 = \frac{\varepsilon_f k_0 M_2 - k(k \cdot M_2)}{k^2 - \varepsilon_f k_0^2} \tag{16}$$

where $\varepsilon_f = \varepsilon_2/\varepsilon_o$ , is the dielectric constant of the magnetic medium. Similarly taking cross product of equation (15), and using equation (14) with the fact $k \cdot E_2 = 0$, yields

$$E_2 = \frac{-\omega \mu_o (k \times M_2)}{k^2 - \varepsilon_f k_0^2} \tag{17}$$

Using this value of $E_2$, equation (14) becomes

$$\nabla \times H_2 = \frac{-i\varepsilon_f k_0^2 (k \times M_2)}{k^2 - \varepsilon_f k_0^2} \tag{18}$$

Now we can consider the magnetostatic range by taking $k >> (\omega/c)(\varepsilon_f)^{1/2}$ . Let us examine equations (16), (17) and (18) in this limit. Since both the numerator and denominator of (16) contain terms quadratic in $k$ , we conclude that $H_2$ remains finite for large $k$ provided $k \cdot M_2 \neq 0$ . In contrast, equations (17) and (18) for $E_2$ and $\nabla \times H_2$ , respectively, vanish as $1/k$ for large $k$. Thus, waves in our magnetic material are described by the following magnetostatic equations,

$$\nabla \times H_2 = 0 \tag{19}$$

$$\nabla \cdot B_2 = 0 \tag{20}$$

Since $H_2$ remains finite, thus an approximation to the electric field may be obtained from

$$\nabla \times E_2 = -i\omega \mu_o \bar{\mu} H_2 \tag{21}$$

where $\bar{\mu}$ is the magnetic permeability tensor (Polder tensor) of the gyromagnetic ferrite (YIG). Equations (19), (20) and (21) comprise the magnetostatic approximation to Maxwell's equations. Waves that are described by these equations are called magnetostatic waves. Magnetic permeability tensor $\bar{\mu}$ of the ferrite (YIG) film is described by Awai et al [10] and Hamada et al [8], and is shown as

$$\bar{\mu} = \begin{pmatrix} \mu_{xx} & i\mu_{xy} & 0 \\ -i\mu_{xy} & \mu_{xx} & 0 \\ 0 & 0 & \mu_{xx} \end{pmatrix} \qquad (22)$$

$\mu_{xx}$ , $\mu_{xy}$ and $\mu_{zz}$ are called the elements of the Polder susceptibility tensor given by

$$\mu_{xx} = \mu_B\left(1 + \frac{f_o f_m}{f_o^2 - f^2}\right)$$

$$\mu_{xy} = \mu_B\left(\frac{f f_m}{f_o^2 - f^2}\right)$$

and $\mu_{zz} = \mu_B$

where $f = \omega/2\pi$ , $f_o = (1/2\pi)\gamma\mu_o H_o$ , $f_m = (1/2\pi)\gamma\mu_o M_o$ and $\mu_B$ is the background permeability and $M_o$ is dc value of saturation magnetization. Now by equation (19) $\nabla \times H_2 = 0$ , which means there exists a magnetic potential $\Psi$ giving $\nabla \times \nabla\Psi = 0$ , i.e. $H_2 = -\nabla\Psi$. Since $B_2 = \bar{\mu} \cdot H_2$ , equation (20) can now be written in the following form

$$\nabla \cdot (\bar{\mu} \cdot \nabla\Psi) = 0$$

Solving this equation, we arrive at the following expression:

$$\frac{\partial^2\Psi}{\partial x^2} = k^2\Psi \qquad (23)$$

The solution of this equation can be written as

$$\Psi = (Ce^{kx} + De^{-kx})e^{i(\omega t - ky)} \qquad (24)$$

Using $H = -\nabla\Psi$, the field components are calculated as

$$H_{x2} = -k(Ce^{kx} - De^{-kx})e^{i(\omega t - ky)} \qquad (25)$$

$$H_{y2} = ik(Ce^{kx} + De^{-kx})e^{i(\omega t - ky)} \qquad (26)$$

Now using, $B_2 = \bar{\mu} \cdot H_2$ , $x$ component of the magnetic field is obtained as

$$B_{x2} = -\mu_0 k\{(\mu_{xx} + s\mu_{xy})Ce^{kx} - (\mu_{xx} - s\mu_{xy})De^{-kx}\}e^{i(\omega t - ky)} \quad (27)$$

From Maxwell equation, we have $E_{z2} = (\omega/k)B_{x2}$ , thus electric field component is given by

$$E_{z2} = -\mu_0 \omega\{(\mu_{xx} + s\mu_{xy})Ce^{kx} - (\mu_{xx} - s\mu_{xy})De^{-kx}\}e^{i(\omega t - ky)} \quad (28)$$

where $s = \pm 1$ defines the propagation of waves in the forward and backward direction. Using the boundary conditions that is equality of the tangential components of the field components $E_z$ and $H_y$ at the interfaces $x = d_1$ and $x = d_2$ . The final dispersion relation is obtained as

$$e^{-2k\Delta d} = \frac{\left[\frac{k}{k_1} + (\mu_{xx} + s\mu_{xy})\right]\left[\frac{k}{k_3} + (\mu_{xx} - s\mu_{xy})\right]}{\left[\frac{k}{k_1} - (\mu_{xx} - s\mu_{xy})\right]\left[\frac{k}{k_3} - (\mu_{xx} + s\mu_{xy})\right]} \quad (29)$$

where $\Delta d = d_2 - d_1$ , is the ferrite film thickness.

## 3. NUMERICAL ANALYSIS OF DISPERSION RELATION AND LIMITING CASES

We numerically solve the dispersion relation (29) for effective wave index $n$ versus propagation frequency $f$. For this purpose we rewrite equation (29) as

$$n_{\pm} = -\frac{1}{2k_o \Delta d} ln \frac{\left[\frac{k}{k_1} + (\mu_{xx} + s\mu_{xy})\right]\left[\frac{k}{k_3} + (\mu_{xx} - s\mu_{xy})\right]}{\left[\frac{k}{k_1} - (\mu_{xx} - s\mu_{xy})\right]\left[\frac{k}{k_3} - (\mu_{xx} + s\mu_{xy})\right]} \quad (30)$$

The $\pm$ stands for the effective wave index corresponding to the forward and backward propagations for $s = \pm 1$. Figure 2 shows the effective wave index $n$ as a function of the propagation frequency, for different values of ferrite film thickness $\Delta d$ and $= \pm 1$ . Parameter values used in the numerical analysis are $\gamma = 1.72 \times 10^{11} s^{-1} T^{-1}$, $\mu_B = 1.25$, $c = 3 \times 10^8 ms^{-1}$, $\mu_o H_o = 0.1T$, $\mu_o M_o = 0.1750T$, $\varepsilon_l = 3$, $\varepsilon_f = 1$, $\varepsilon_c = -40$, $\sigma = 45 \times 10^6 \Omega^{-1} m^{-1}$ and frequency ranges from $4\ to\ 6\ GHz$. Other values are given in Figure 2

captions. These values have been used in the papers by Hamada et al [4, 8], and O'Keeffe & Patterson [6].

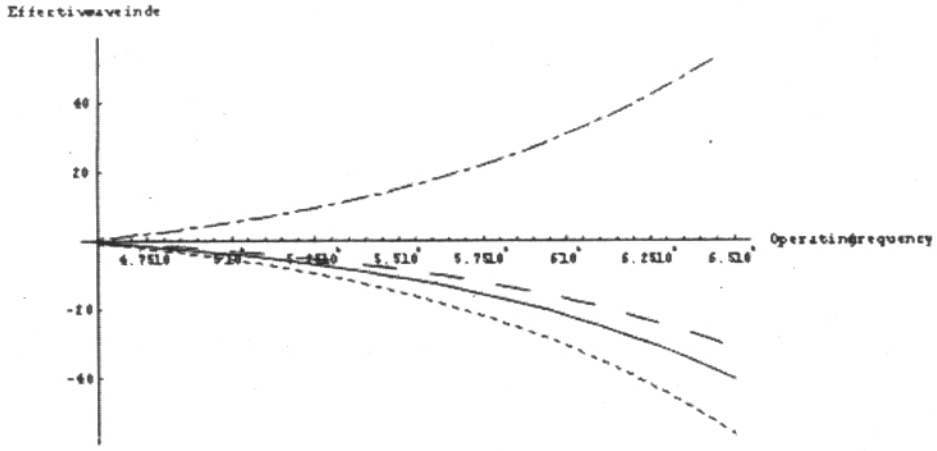


Figure 2. Frequency $f$ versus effective wave index $n$ for different values of ferrite film thickness $\Delta d$. for $s = 1$, and $\Delta d = 50\mu m$ (----------), $\Delta d = 70\mu m$ (——————), $\Delta d = 90\mu m$ (— — —)

for $s = -1$, and $\Delta d = 50\mu m$ (- - - - - -), $\Delta d = 70\mu m$ (—— ——), $\Delta d = 90\mu m$ (——————)

It can be observed from Figure 2 that the effective wave index shows a similar sensitive reciprocal behavior to the ferrite film thickness for forward and backward directions.

Figure 3 shows the phase shift $\Delta n = n_+ - n_-$ as a function of the film thickness $\Delta d = d_2 - d_1$, for the different values of frequencies. It is clear that waveguide structure shows

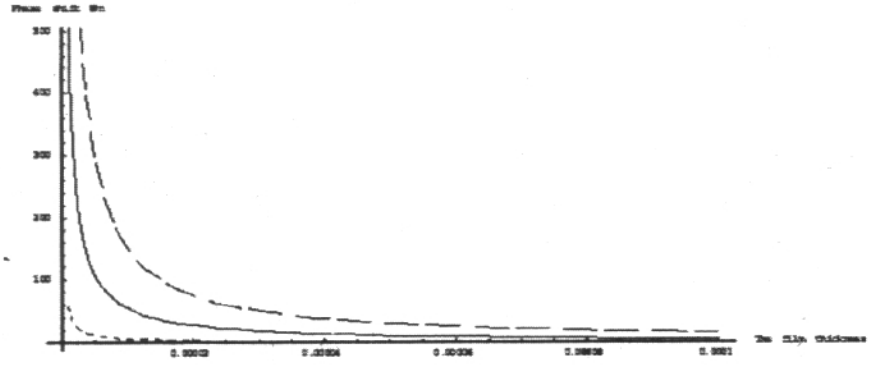

Figure 3. Phase shift $\Delta n$ versus ferrite film thickness $\Delta d$, for different values of frequency $f$, for $f = 4.6GHz$ (----------), $f = 5GHz$ (——————), $f = 5.5GHz$(— — — —)

the non-reciprocal behaviour on increasing the film thickness. Thus the reciprocal behaviour can be controlled by adjusting the film thickness and the propagation frequency, which is similar to the case of Hamada et al. [8].

## 4. LIMITING CASES

In the first limiting case, we take wave numbers $k_1$ and $k_3$

$$k_1 = \sqrt{k_0^2(n^2 - \varepsilon_l)}$$

$$k_3 = \sqrt{k_0^2(\frac{i\sigma\omega\mu_o}{k_o^2} + n^2 - \varepsilon_c)}$$

For a poor conductor $\sigma = 0$ , and using the approximation for the wave numbers $k >> (\omega/c)(\varepsilon_l)^{1/2}$ and $k >> (\omega/c)(\varepsilon_c)^{1/2}$ , we have $k_1 = k_3 = k$, our dipersion relation reduces to

$$e^{-2k\Delta d} = \frac{[1+(\mu_{xx}+s\mu_{xy})][1+(\mu_{xx}-s\mu_{xy})]}{[1-(\mu_{xx}-s\mu_{xy})][1-(\mu_{xx}+s\mu_{xy})]}$$

This is well known expression of Damon-Eshbach surface wave mode for tangentially magnetized ferrite film [11]. In a simple form this can also be written as

$$f^2 = f_o(f_o + f_m) + \frac{f_m^2}{4}(1 - e^{-2k\Delta d})$$

For the numerical analysis, the above relation can be written as

$$n = -\frac{1}{2k_o\Delta d} ln\left[1 - \frac{4}{f_m^2}\{f^2 - f_o(f_o + f_m)\}\right] \quad (31)$$

Figure 4 shows the plot of effective wave index versus propagation frequency for different value of film thickness. In this case of a poor conductor, the dependence on reciprocal

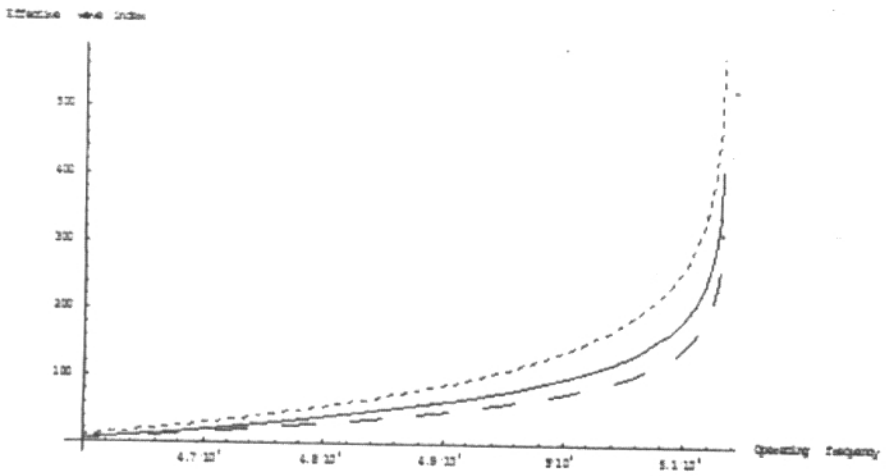

Figure 4. Frequency $f$ versus effective wave index $n$ for different values of ferrite film thickness $\Delta d$. for case 1, $\Delta d = 50\mu m$ (---------- ), $\Delta d = 70\mu m$ (—————— ). $\Delta d = 90\mu m$ (— — — )

behaviour has vanished. In the second limiting case, for infinite conductivity we take $\sigma = \infty$ and boundary conditions for the interface $x = d_1$ are $H_{y2} = H_{y3} = 0$ and $E_{z2} = E_{z3} = 0$ , using these conditions and after skipping some algebra, we get the following dispersion relation

$$e^{-2k\Delta d} = -\frac{[k(\mu_{xx}+s\mu_{xy})]+[k_1\mu_v\mu_{xx}]}{[k(\mu_{xx}-s\mu_{xy})]-[k_1\mu_v\mu_{xx}]}$$

where $\mu_v = \frac{\mu_{xx}^2-\mu_{xy}^2}{\mu_{xx}}$ is called the Voigt permeability [11].

The above expression can be written as

$$n = -\frac{1}{2k_o\Delta d}\, ln\frac{\left(\mu_{xx}+s\mu_{xy}\right)+\mu_v\mu_{xx}}{\mu_v\mu_{xx}-\left(\mu_{xx}-s\mu_{xy}\right)} \tag{32}$$

Figure 5 shows the effective wave index $n$ as a function of the propagation frequency $f$, for different values of film thickness. This shows that there exists an asymptotic behaviour for backward propagation at certain frequency showing a large value of effective wave index.

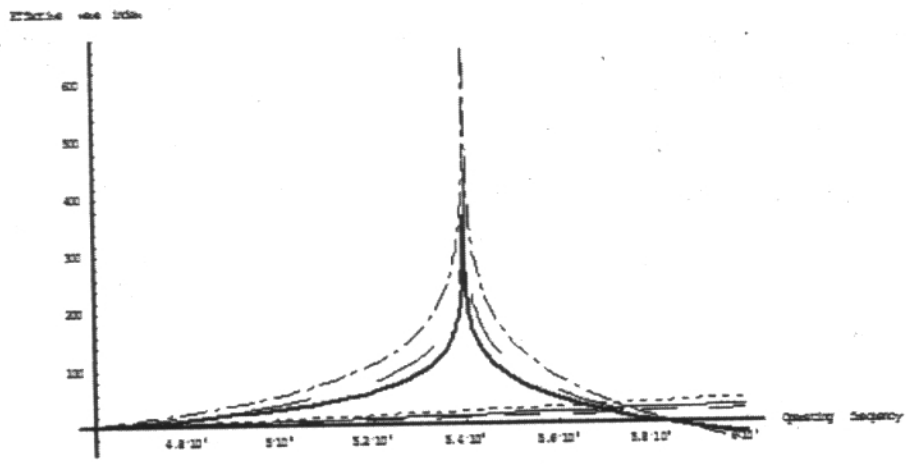

Figure 5. Frequency $f$ versus effective wave index $n$ for different values of ferrite film thickness $\Delta d$, for case 2, and $s = 1$, and $\Delta d = 50\mu m$ (---------), $\Delta d = 70\mu m$ (————), $\Delta d = 90\mu m$ (— — —) for $s = -1$, and $\Delta d = 50\mu m$ (– – – –), $\Delta d = 70\mu m$ (—— ——), $\Delta d = 90\mu m$(————)

## 5. CONCLUSIONS

The magnetostatic surface waves in a layered waveguide structure consisting of a linear dielectric, ferrite film and a conductor have been investigated. The dispersion relation is obtained and dependence of effective wave index on the propagation frequency has been examined. Reciprocal behaviour is observed in the dispersion characteristics. We have also investigated the phase shift versus film thickness for waves propagating in two directions for different values of frequencies, showing non-reciprocal behaviour on increasing the film thickness. In the limiting case of a poor conductor, the dependence on reciprocal behavior has vanished and we get an expression of Damon-Eshbach surface wave mode for ferrite film. In the second limiting case, there exists an asymptotic behaviour for backward propagation at certain frequency showing a large value of effective wave index.

**Acknowledgement:** This work was conducted under the Pakistan Science Foundation (P.S.F.) Research Grant No. PSF/Res/P-PU/Phys(131).

## REFERENCES


1. A.D. Boardman, M. Bertolotti and T. Twardowski, *Non Linear Waves in Solid State Physics*,1990, Plenum Press, New York.

2. M. M. Shabat and J. Plezl, Infrared Physics & Technology, **37**, 265 (1996).

3. A.D. Boardman, M. M. Shabat and R. F. Wallis, J. Phys. D: Appl. Phys. **24**, 1702 (1991).

4. M.S. Hamada, M. M. Shabat and D. Jager, The Islamic University Journal, **14**, 51 (2006).

5. M.S. Hamada, M. M. Shabat, M. M. Abd Elaal and D. Jager, Journal of Superconductivity:Incorporating Novel Magnetism, **16**, 443(2002)

6. T. W. O'Keeffe and R. W. Patterson, J. Appl. Phys. **49**, 4886 (1978).

7. A. A. Semenov, S. F. Karmanenko, A. A. Melko, A. V. Bobyl, R. A. Suris, Yu, M. Gal'perin and T. H. Johansen, Technical Physics, **46**, 1218 (2001).

8. M.S. Hamada, A.I. Assad, H. S. Ashour and M. M. Shabat, Journal of Microwave and Optoelectronics, **5**, 45 (2006).

9. Daniel D. Stancil, *Theory of Magnetostatic Waves*, 1993, Springer-Verlag.

10. I.Awai, K. Ohtsuki and J. Ikenoue, Japanese Journal of Applied Physics, **15**, 1305 (1976).

11. Michael G. Cottam and David R. Tilley, *Introduction to Surface and Superlattice Excitations*, 1989, Cambridge University Press.

PK ISSN 0022-2941; CODEN JNSMAC
Vol. 47, Nos. 1 & 2 (April & October 2007) PP-25-32

# DIELECTRIC PROPERTIES OF NOVEL POLYESTER COMPOSITE MATERIAL

**E.H. AWAN AND A. SHAMIM**
Department of Physics, GC University, Lahore-54000, Pakistan.

**ABSTRACT:** The purpose of this study is to improve the dielectric properties of composites consisting of unsaturated polyester, sand and $CaCO_3$. Frequency and temperature dependence of dielectric constant and tangent loss in polyester composite with various compositions of unsaturated polyester, filler and $CaCO_3$ are studied by varying the frequency ( 30, 50, 100 Hz, 100 KHz and 300 KHz) and temperature (30, 50, 70, 90 and 120°C). Results reveal that the dielectric constant and tangent loss are increased with the increase in concentration of filler. Moreover, the maximum value of dielectric constant and dielectric loss is observed at 120 °C for the low value of frequency 50 Hz. showing the major contribution to the electric polarization is due to orientation polarization. The dielectric constant and tangent loss also increases with increasing temperature because of greater movement of the dipole molecular chains within the polyester at high temperature.

## 1. INTRODUCTION

Porcelain insulators have been widely used since long because of their good insulating qualities and comparatively low preparation cost. But with the passage of time, as the cost of fuel increased so did the manufacturing cost of porcelain insulators. Interest in polymer composites has increased many folds in recent years because they are light weight, comparatively cheaper and are used in capacitors as dielectric medium [1-4]. The most attractive property of polymeric composites is that their dielectric properties can be changed substantially by choice of shape, size and the conductivity by filler in matrix. Polymer concrete could be used as an overlay in pavement, bridges, and runways or in pre-cast applications such as transportation, and hydraulic components of machines [5]. Polymer composite insulators are finding increasing application for outdoor use at both transmission and distribution levels of electricity [6].

The investigations show that the samples containing 50/50 polypropylene-phthalate-hexane-maleate(PE1) / poly[axydiethylene-phthalate-hexane-maleate] (PE2) loaded with 60-70% clay posses the most promising dielectric properties. The quartz composite 60% had the best mechanical properties with respect to the clay and calcium carbonate[7].The compressive strength decreases with an increase in sand/clay, as well as the styrene content in the unsaturated polyester resin whereas the apparent porosity and water absorption of the composite sample increases[8]. The replacement of 15% by weight of sand with fly ash improves the compressive strength of unreinforced PC cylinders by about 30% and the flexural strength of steel-reinforced PC beams by about 15%. Other improvements in properties are

relatively minor and include the tensile bond strength of PC under thermal cycling and the creep compliance of the PC under sustained loading. The replacement of sand with fly ash, however, does not seem to have an impact on the shear strength of PC. Potential applications of PC using fly ash are numerous, including thin overlays on bridges and floors, repairing concrete bridges and pavements, and the production of precast components such as wall panels, floor blocks, and underground vaults[9].

In this article we present the effect of filler on dielectric properties of the composites. Results depend on the type of filler and its concentration in the sample along with temperature and frequency of A.C.

## 2. EXPERIMENTAL PROCEDURE

**Specimen preparation**

The materials used for specimen preparation are commercially available. The specimens are prepared by using unsaturated polyester, calcium carbonate and natural sand collected from the bed of river 'Ravi'. The composition of the samples is given below in Table1. A special technique known as *master batching* was used for mixing the calcium carbonate, sand and polyester resin [10]. The mixture of calcium carbonate, sand, cobalt and methyl ethyl ketone peroxide (MEKP) was carefully poured into the mould and pressed at five ton pressure in order to avoid air gaps. All the samples were cured at room temperature for one day. The prepared specimens were baked in an oven at 50 °C for 1 hour. In the end, all specimens were ground and polished for characterization.

| Sample No. | Name of material | %Weight |
|---|---|---|
| A. | Calcium carbonate | **80** |
| | Sand | **20** |
| | Polyester | **35%** of mixture of $CaCO_3$ and Sand. |
| B. | Calcium carbonate | 60 |
| | Sand | 40 |
| | Polyester | 35% of mixture of $CaCO_3$ and Sand. |
| C. | Calcium carbonate | 40 |
| | Sand | 60 |
| | Polyester | 35% of mixture of $CaCO_3$ and Sand |
| D. | Calcium carbonate | 20 |
| | Sand | 80 |
| | Polyester | 35% of mixture of $CaCO_3$ and Sand |

**Table 1: Composition of samples for determination of dielectric constant and tangent loss**

For the determination of dielectric constant and tangent loss, Electric Loss Measuring Set TRS-10 is used. The dependence of the electric constant and tangent loss of the specimen is

measured at different frequencies and temperatures ranging from 30 Hz to 100 kHz and 30°C to 120°C, respectively. The results are presented in Fig. 1 and Fig. 2.

## 3. RESULTS AND DISCUSSION

The dielectric constant and dielectric loss of samples are determined as follows:

$$\text{Dielectric constant } \epsilon = \frac{C_x}{C_o}$$

Where $C_x$ (pF) is measured capacitance and $C_o$(pF) is calculated using the formula

$$C_o = \frac{0.0885 \times A}{t}$$

Where "A ($cm^2$)"is the area of electrode and "t(cm)" is the thickness of the sample.

The dielectric loss is given by $\tan\delta = \frac{G_x(S)}{\omega C_x(F)}$ Where $\omega = 2\pi f$

"f" is the measuring frequency and $G_x = G_R(R-R_o)$ [11].

A comparison of Fig.(1a),(1b), (1c) and (1d) elaborates that the dielectric constant is higher for the specimen having higher concentration of filler under identical frequency and temperature. Similarly, the comparison of Fig.(2a),(2b),(2c) and (2d) shows that the tangent loss is higher for higher concentration of filler under identical temperature and frequency due to orientation polarization, but this increase is small at high frequency of 100 KHz and large at temperature of 120°C. If the temperature is kept constant, it can also be concluded from the graph that the dielectric constant decreases with increase in frequency for all three specimens. However, the decrease is more pronounced in specimen of higher concentration of filler and becomes progressively less pronounced with a decreasing concentration of filler.

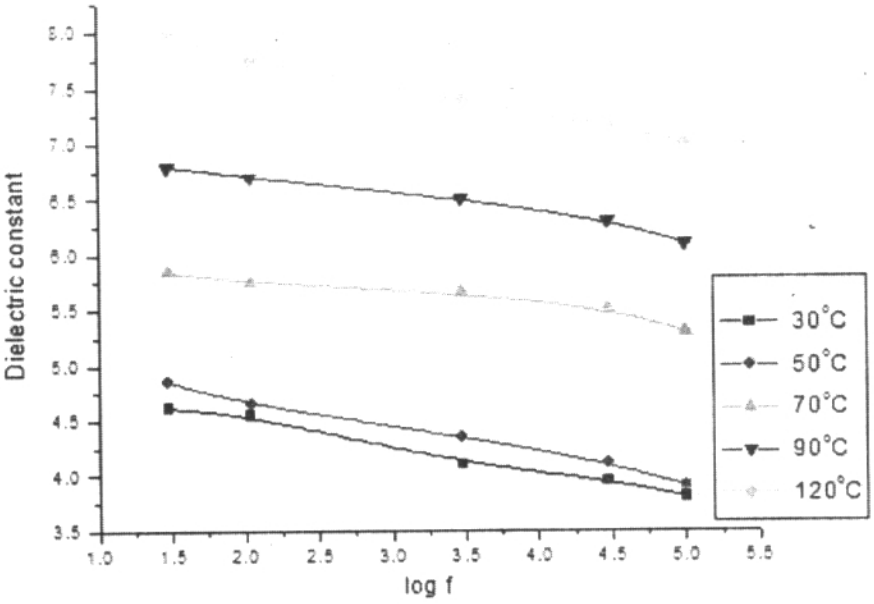


Fig. 1a. Graph between log f and dielectric constant for specimen A

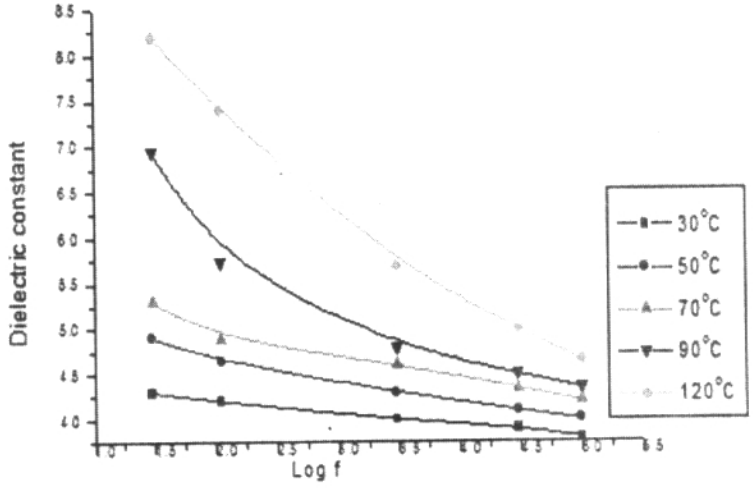


Fig. 1b: Relation between dielectric constant and frequency at various temperatures for specimen "B".

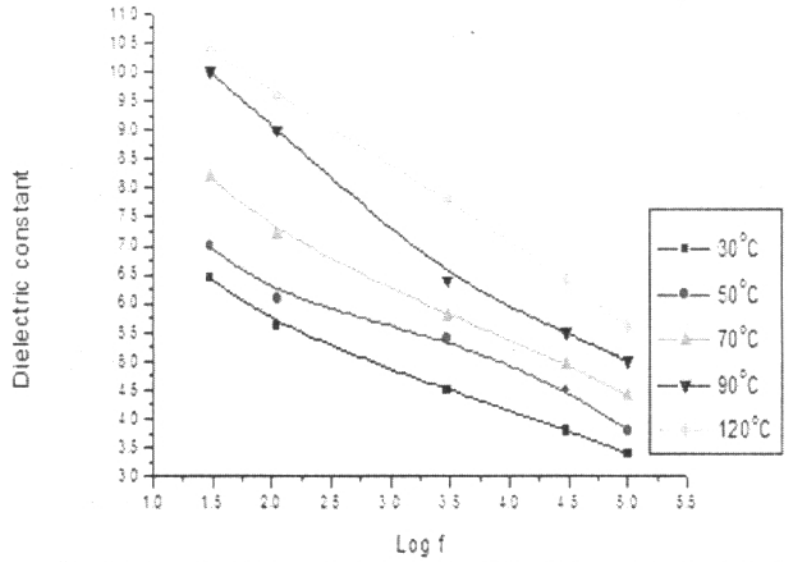


Fig. 1c: Relation between dielectric constant and frequency at various teperatures for specimen "C".

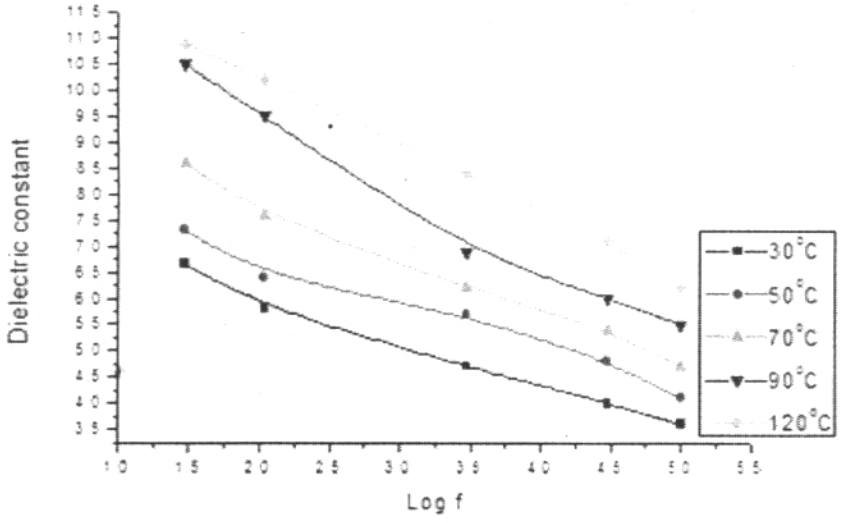


Fig. 1d: Relation between dielctric constant and frequency at varicus temperatures for specimen "D

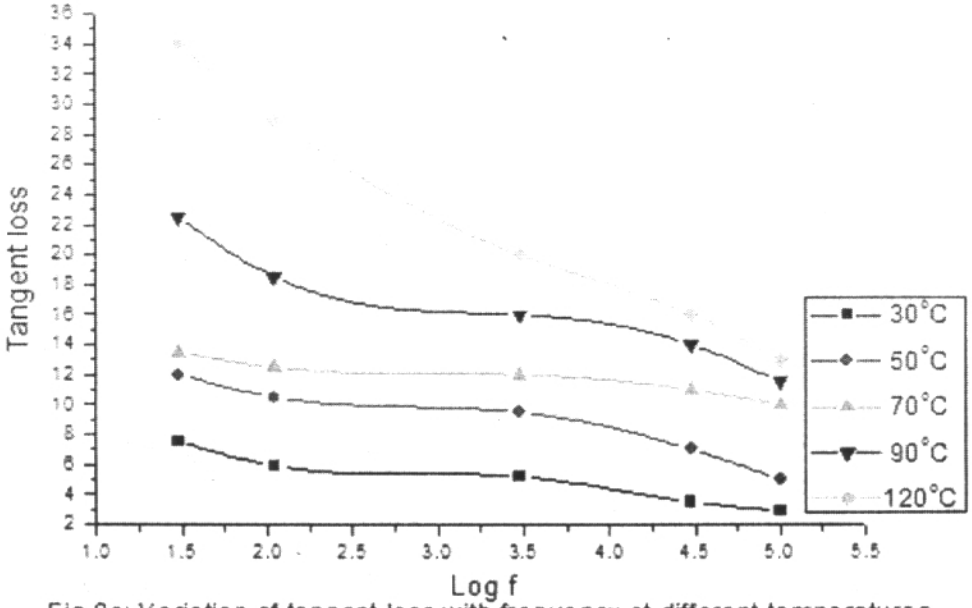


Fig 2a: Variation of tangent loss with frequency at different temperatures.

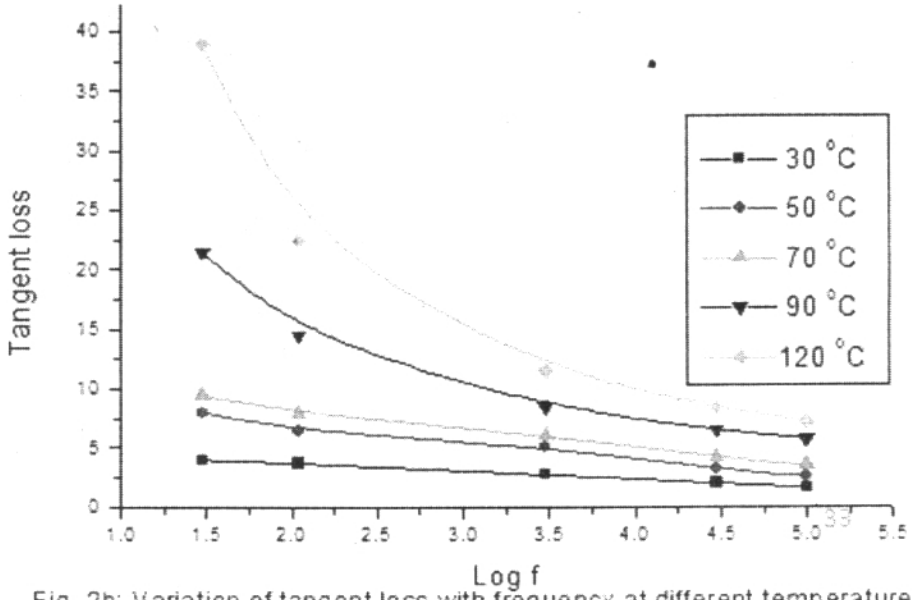


Fig. 2b: Variation of tangent loss with frequency at different temperatures.

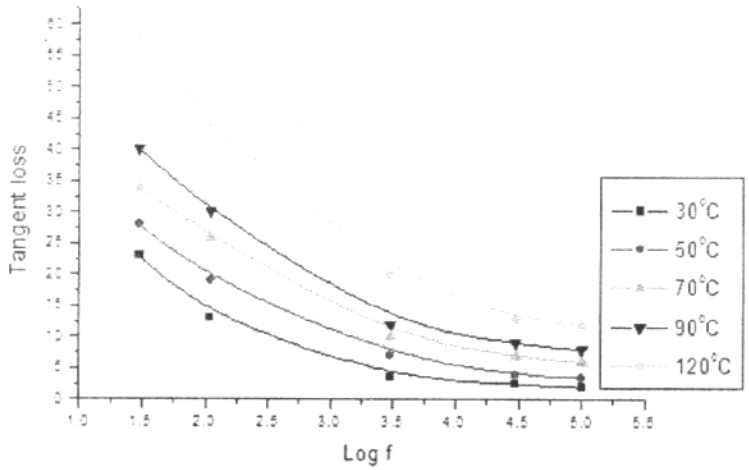


Fig. 2c: Relation between tangent loss and frequency at various temperatures for specimen "C".

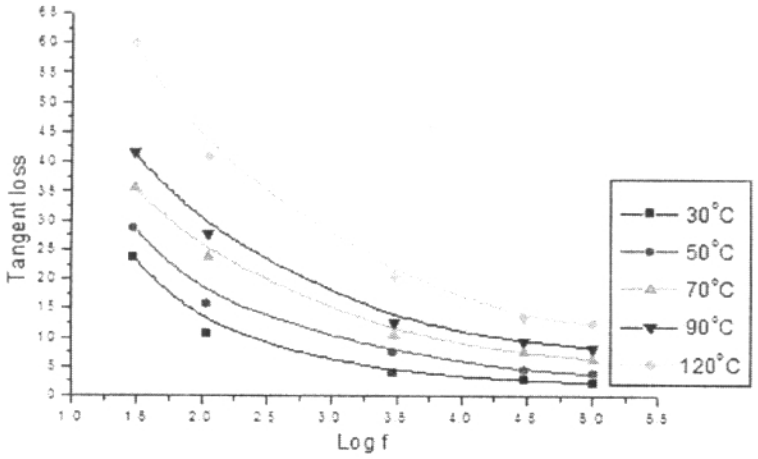


Fig. 2d: Relation between tangent loss and frequency at various temperatures for specimen "D".

It is also studied that for all these specimens at a constant frequency the electric constant increases with the increasing temperature. Thus we can say that the effect of temperature and concentration of filler (sand) work in the same direction.

The comparison of Fig.(2a),(2b),(2c) and (2d) shows that the value of tangent loss decreases with increase in frequency of A.C. signal for all of the specimens A, B, C and D. It is usual behavior of most materials [12]. The value of tangent loss increases to high values at higher

temperature with decreasing frequency. It is due to structural relaxation which promotes orientation polarization at higher temperature and lower frequency. This effect is maximum at 120°C. The curves show that the composition of a specimen also influences the value of tangent loss. When the amount of filler (sand) is increased the value of tangent loss is also increased.

## 4. CONCLUSIONS

It is observed that the increase in the concentration of filler results in an increasing dielectric constant and tangent loss. The effect of increase in concentration of filler is more pronounced at lower frequency and higher temperature, showing that the orientation polarization placed a very important role in determining dielectric properties of polyester concrete specimens. The dielectric constant and dielectric loss increases with increase of temperature of the sample due to greater freedom of movement of the dipole molecular chains within the polyester at high temperature.

## REFERENCES

1. Nobuyoshi Awaya, Hiroshi Inokawa, Eiichi Yamamoto, Yukio Okazaki, Masayasu Miyake, Yoshinobu Arita and Toshio Kobayashi, IEEE Trans. Electron Devices, **43**(1996), 1206.
2. M. Akram, A.Javed and T. Z. Rizvi, Turk J. Phys **29** (2005), 355 -365.
3. J. H. Golden, C. J. Hawker and P. S. Ho, Designing Porous Low-k Dielectrics (Semiconductor International, 2001).
4. Ronald J. Gutmann, IEEE Trans. Microwave Theory Tech, **47**, (1999), 667.
5. K. S. Rebeiz, M. Asce and A. P. Craft J, Energy Engrg. **128**(2002) 62-73.
6. M. Ehsarti and H. Borsi,...2004 International conference of Solid Dielectrics, Toulouse, France, July 5-9. 2004.
7. S. H. Mansour and S. L. Abd-El- Messeih J. of Appl Polym Sci **83**(2002) 1167-1180.
8. M. R. Ismail, M. A. Ali, A. A. El-Milligy and M. S. Afifi J. of Appl Polym Sci **72**(1999) 1031-1038.
9. K. S. Rebeiz, M.Asce; S. P. Serhal and A. P. Craft J. Mat. in Civ. Engrg., **16** (2004) 15-19.
10. Composite polymeric materials by R. P. Sheldon Applied Science, published in London and New York (1982).
11. Manual " Electric Loss Measuring Set TRS-10T",Japan.
12. C.P. Smyth "Dielectric Behaviour and Structure" New York, McGraw Hill (1995).

PK ISSN 0022-2941; CODEN JNSMAC
Vol. 47, Nos. 1 & 2 (April & October 2007) PP-33-41

# PREFERENCE ESTIMATION OF AMINO ACIDS IN THE VICINITY OF EGFR ACCEPTOR PHOSPHOTYROSINE USING COMPUTATIONAL METHOD

WAJAHAT M. QAZI[1], KHALIL AHMAD[2] AND TAYYABA WAJAHAT[3]
[1]Department of Physics, G.C. University, Lahore. Pakistan
[2]School of Computer Science, NCBA & E, Lahore, Pakistan
[2]AZAM Education Foundation, Lahore, Pakistan

**ABSTRACT:** Protein phosphorylation is an important post-translational modification which plays an important role in regulating protein's structure and function. Protein phosphorylation is regulated and catalyzed by Kinases. Number of prediction models have been developed to predict modification potential for various Kinase-based phosphorylation. All these reported models are based data learning strategy. They do not take into account the presence, absence, and their preferences while learning correlation patterns within adjacent amino acids. Knowledge of presence and absence of specific residues along with their preferences in the vicinity of modification site (acceptor residue) may help in the development of better prediction models. This study performs preference estimation for phosphorylated and non-phosphorylated Tyr which has the potential to get modified by EGFR Kinase. Result of this analysis reveals 3 significantly preferred amino acids for EGFR-based phosphorylated Tyr and 10 significantly preferred amino acids for non-phosphorylated Tyr.

## 1. INTRODUCTION

Proteins undergo a number of biological processes as soon as they are translated from genetic information. These biological processes include co- and/or post- translational modifications. These post-translational modifications (PTMs) generally result as the outcome of docking of functional groups on acceptor residues. Studies have reported that PTMs like phosphorylation, glycosylation etc are responsible for regulating protein functional activities by inducing changes in their 3D conformation [1, 2].

Large number of bioinformatics algorithms based on machine learning techniques have been reported to analyze these PTMs. Indeed, they help in predicting modification potential of the target substrate but do not reveal preference of amino acids in the vicinity of target residues. Few efforts were made in the past to estimate preference of the amino acids in the vicinity of glycosylated [3] and phosphorylated proteins [4]. Analysis of glycosylated proteins revealed some important information like Pro at position -1 and/or +3 have positive and strong preference in the vicinity of glycosylated substrate and may play an important structural role in regulating *O*-glycosylation [3]. Another study on protein phosphorylation was performed to reveal preferred amino acids [4]. In this study [4], phosohorylated and non-phosphorylated sites were marked separately in the amino acids sequence as pseudo-amino acids. These pseudo-amino acids were PS, PT, PY for phosphorylated Ser, Thr and Tyr, respectively; similarly NPS, NPT and NPY for non-phosphorylated Ser, Thr and Tyr. This study has revealed some important amino

acids which may play significant role in phosphorylation of proteins but did not consider protein Kinases.

Protein phosphorylation of target residues (Ser, Thr and Tyr) is performed by Kinases. Kinases catalyze phosphorylation process [5, 6]. The crystallization studies report that the vicinity of seven to twelve neighboring amino acids around the target substrate are important for Kinase activity [7]..

This study intends to perform preference estimation analysis for EGFR Kinase targeted phosphorylated Tyr and non-phosphorylated Tyr.

## 2. METHODS

Phosphobase.ELM version 3.0 [8] was used as the data source for study. Phosphobase.ELM contained 4252 experimentally verified phosphorylation entries for 1663 proteins [4] and total 225 Kinases. Phosphorylation data of phospho-tyrosine associated with EGFR Kinase was filtered out from Phosphobase.ELM version 3.0. This separation process resulted into 50 instances. Data preprocessing was then applied on these 50 instances. The purpose of this data preprocessing was to ensure that there is no inconsistency, error or duplication in these 50 instances. Protein with accession No. P19174 contained duplicate entry for position No.1253. One copy of this duplicate entry was removed. Hence data processing resulted into 49 phsophorylation sites for 24 proteins. These entries were then used to extract entries for non-phosphorylated sites. In this process, all other sites in these 24 proteins, which are not experimentally known for Tyr, in Phosphobase.ELM, were treated as non-phosphorylated sites. This extraction process resulted into 384 non-phosphorylated sites. Statistics for phosphorylated and non-phosphorylated sites are summarized in Table 1.

Peptides were extorted from the protein sequences using the position information given in respective dataset (i.e. phosphorylated and non-phosphorylated). This process resulted into 49 peptides in phosphorylated dataset and 384 peptides in non-phosphorylated dataset. The size of the peptide was 21 amino acids (i.e. 10 amino acids in the right and 10 amino acids in the left side of the target residue) in both groups.

Preference estimation procedure was applied separately on both groups i.e. phosphorylated and non-phosphorylated Preference estimation was performed using computational method reported in [3,4,9]and same is discussed here. The method computes following 6 computation quantities.

1. **Observed Frequency (OF)**

$F_{observed}(X)_p = \frac{\sum N_{observed}(X)_p}{m}$, where $N_{observed}(X)_p$ was the observed count for the amino acid X at position p and m was the total number of peptides in respective groups.

2. **Expected Frequency (EF)**

$F_{expected}(X) = \frac{\sum_{i=1}^{n} N_i(X)}{\sum_{i=1}^{n} T_i}$ , $N_i(X)$ was the number of residues of type X in protein i, $T_i$ was the total number of amino acids in protein i, and n was the total number of proteins in respective groups.

3. **Expected Count (EC)**

$N_{expected}(X) = mF_{expected}(X)$, as mentioned above

4. **Deviation Parameter (DP)**

It was used as the normalization parameter to estimate the preference of amino acids in the vicinity of target amino acid/group. If the value of deviation parameter is positive for particular amino acid of Type X at position p, then the amino acid was considered as positively preferred. If the value is negative then it was considered as negatively preferred. Expression to compute deviation parameter was:

$$DP(X)_p = \left( \frac{F_{observed}(X)_p - F_{expected}(X)}{F_{expected}(X)} \right) \times 100$$

5. **Statistical Significance of Preference**

The statistical significance of preference based on deviation parameter was estimated by taking the difference between the observed and expected counts i.e. $N_{observed}(X)_p - N_{expected}(X)$ and the values of $\sigma$ for each amino acid X at position p as given below:

$$\sigma = \sqrt{N_{observed}(X)_p}$$

The criterion for the significance was that: If the difference between the observed and expected counts $N_{observed}(X)_p - N_{expected}(X)$ is $\geq 2\sigma$ at a particular position, the deviation parameter value at that position for the amino acid is considered to be statistically significant.

Above mentioned data preprocessing, extraction processes of non-phopshorylated sites, peptide extortion and computational methodology for preference estimation was programmed using, Microsoft C# 2.0 using Microsoft Visual Studio 2005 (Express Edition).

## 3. RESULTS

This study reported the preference estimation analysis around the Tyr which is phosphorylated by EGFR and Tyr residues with are not phosphorylated. The preference estimation on both groups resulted into 3 significant positively preferred (s-preferred) sites for positively phosphorylated peptides and 10 for non-phosphorylated peptides (see Table 1). Detailed results from these two groups are discussed below:

| | Positively Phosphorylated | Non- Phosphorylated | Total |
|---|---|---|---|
| Number of Peptides/Sites | 49 | 384 | 433 |
| Number of S-Preferred Residues | 3 | 10 | 13 |

**Table 1: Preference Statistics**

### Positively Phosphorylated Sites:

Total 49 peptides were analyzed in this group and 3 residues were found to be significantly preferred in the vicinity (see Table 1). The observed frequencies of most frequent amino acids at each position between -10 to +10 are summarized in Table 2.

| Amino Acids | Position | Observed Frequency % |
|---|---|---|
| Ala | -10 | 18.3673469387755 |
| Pro | -9 | 14.2857142857143 |
| Asp | -8 | 12.2448979591837 |
| Asp | -7 | 14.2857142857 |
| Thr | -7 | 14.2857142857 |
| Gly | -6 | 20.4081632653 |
| Asp | -5 | 14.2857142857 |
| Glu | -4 | 18.3673469388 |
| Glu | -3 | 22.4489795918 |
| Asp | -2 | 16.3265306122 |
| Ser | -2 | 16.3265306122 |
| Glu | -1 | 14.2857142857 |
| Val | 1 | 24.4897959184 |
| Glu | 2 | 18.3673469388 |
| Pro | 3 | 16.3265306122 |
| Pro | 4 | 16.3265306122 |
| Pro | 5 | 16.3265306122 |
| Ser | 6 | 18.3673469388 |
| Pro | 7 | 14.2857142857 |
| Lys | 8 | 16.3265306122 |
| Pro | 9 | 14.2857142857 |
| Ser | 10 | 20.4081632653 |

**Table 2: Most Frequent Residues in Positively Phosphorylated Group at Respective Positions between -10 to 10**

It was observed that Ala, Asp, Glu, Gly, Lys, Pro, Ser, Thr, Val were the most frequently occurring amino acids at various positions in the vicinity of targeted Tyr (Table 2). Asp and Thr were found to have same frequency level of 14.2857142857% at same position i.e. -7. Similarly, at position -2, Asp and Ser has same frequency level i.e. 16.3265306122%. It was also observed that Val is the most frequent amino acid in the vicinity of targeted Tyr, with frequency value equal to 24.4897959184%.

Among these frequent amino acids (summarized in Table 2) Gly, Glu and Val were found to be significantly preferred at position -6, -3 and 1, respectively. Observed frequency of these preferred amino acids with their positions is summarized in Table 3.

| Amino Acids | Position | Observed Frequency |
|---|---|---|
| Gly | -6 | 20.4081632653061 |
| Glu | -3 | 22.4489795918367 |
| Val | 1 | 24.4897959183673 |

**Table 3: Frequencies of Significantly Preferred Amino Acids in Positively Phosphorylated Group**

It was noted that Ser at position +10 and Gly at position -6 had same observed frequency values. Moreover, they both are most frequent at their respective position, but Ser at position 10 was not found to be preferred; whereas Gly at position -6 was preferred (see Table 4.). It was found that following amino acids: Ala, Cys, Phe, Gly. His. Ile. Lys. Leu. Met. Asn. Gln. Arg. Ser. Thr. Trp. Tyr, were found to be absent at various positions in the vicinity i.e. their observed frequency was zero (see Table 4). Among these amino acids, Trp was found to be absent at 17 positions, Cys and Tyr were absent at 13 positions, His at 9 positions, Met at 8 positions, Ile at 7 positions. Whereas, Gly, Lys and Gln were found to be absent at 4 different positions. Similarly, Thr and Leu were absent at 3 positions and Phe, Asn and Ser were absent at 2 different positions. Absent, preferred and frequent amino acids are summarized in Table 4.

| AA | -10 | -9 | -8 | -7 | -6 | -5 | -4 | -3 | -2 | -1 | 1 | 2 | 3 | 4 | 5 | 6 | 7 | 8 | 9 | 10 |
|---|---|---|---|---|---|---|---|---|---|---|---|---|---|---|---|---|---|---|---|---|
| Ala | F | | | | | | | | | | | | | | | X | | | | |
| Cys | X | X | | X | X | | X | X | X | | | | X | X | | X | X | X | X | |
| Asp | | | F | F | | F | | | F | | | | | | | | | | | |
| Glu | | | | | | | F | F | | F | | F | | | | | | | | |
| Phe | | | | | | X | | | | | X | | | | | | | | | |
| Gly | | | | | F | | | | | | | X | X | X | X | | | | | |
| His | | | X | | | X | | X | X | | | X | | X | X | X | X | | | |
| Ile | | X | | | X | | X | X | X | | | | | | | | | X | | X |
| Lys | | | | | | | | | X | X | X | | | X | | | | F | | |
| Leu | | | | | | | | | X | | | X | | | | | | | | X |
| Met | | | X | X | | | X | X | X | | | | | X | X | | | | X | |
| Asn | X | | | | X | | | | | | | | | | | | | | | |
| Pro | | F | | | | | | | | | | | F | F | F | | F | | | |
| Gln | | | | X | | X | | | | X | | | | | | | | X | | |
| Arg | | | | | X | | | | | | | | | | | | | | | |
| Ser | | | | | | | | | F | | X | | | | X | | | | | F |
| Thr | | | | F | | | | X | | | X | | | | | X | | | | |
| Val | | | | | | | | | | | F | | | | | | | | | |
| Trp | X | | X | X | X | X | X | X | X | X | X | X | X | X | X | | X | X | | X |
| Tyr | X | | | X | X | X | X | | X | X | X | X | | | | X | X | X | | X |

| | |
|---|---|
| X | Represents those Sites where the corresponding Amino Acid at the corresponding Position is absent |
| F | Represents those Sites where the corresponding Amino Acid at the corresponding Position is Most Frequent |
| F | Represents those Sites where the corresponding Amino Acid at the corresponding Position is Most Frequent and Significantly Preferred |

**Table 4: Positively Phosphorylated Group Non-Phosphorylated Sites**

Preference estimation was performed on 384 peptides (see Table 1). These instances represented the peptides which were not phosphorylated by EGFR Kinase. Preference estimation resulted into 10 significantly preferred residues. These significantly preferred residues are summarized in Table 5 along with their respective observed frequencies. It was observed

that on few of the positions in the vicinity of non-phosphorylated Tyr, had more than one significantly preferred residues.

These positions are -9 with Phe and Tyr as preferred amino acids and -3 with Lys and His as preferred amino acids. It was noted that Phe at position -9 is the most frequent amino acid among the preferred ones, with observed frequency of 7.291666. Observed frequency range for preferred residues was between 2.864 and 8.59.

| Amino Acids | Position | Observed Frequency |
|---|---|---|
| Phe | -9 | 7.29166666667 |
| Tyr | -9 | 5.20833333333 |
| Ile | -7 | 7.03125 |
| Phe | -4 | 6.51041666667 |
| Lys | -3 | 9.375 |
| His | -3 | 4.94791666667 |
| Trp | -1 | 2.86458333333 |
| Ile | 2 | 7.03125 |
| Arg | 5 | 8.59375 |
| Gln | 8 | 8.59375 |

**Table 5: Frequencies of Significantly Preferred Amino Acids in Non- Phosphorylated Group**

Most frequent amino acids in the vicinity of non-phosphorylated Tyr along with their respective observed frequency are summarized in Table 6. Details of these most frequent amino acids are given as: Leu was found to be most frequent at 10 different positions, Glu and Ser were found to be most frequent at 4 different positions and Ala was found to be most frequent at 2 different positions (see Table 7).

It was observed that amino acids with observed frequency values greater than 9.6 were not significantly preferred (see Table 5 and Table 6). It was also observed that His at position -2, Trp at position -7 and -3 were found to absent in the vicinity i.e. their observed frequency was zero. (see Table 7).

| Amino Acids | Position | Observed Frequency |
|---|---|---|
| Leu | -10 | 9.63541666667 |
| Leu | -9 | 11.9791666667 |
| Glu | -8 | 10.15625 |
| Leu | -7 | 11.1979166667 |
| Leu | -6 | 9.63541666667 |
| Glu | -5 | 8.59375 |
| Leu | -4 | 10.15625 |
| Leu | -3 | 10.6770833333 |
| Ser | -2 | 9.63541666667 |
| Leu | -1 | 8.85416666667 |
| Ser | 1 | 9.89583333333 |
| Glu | 2 | 10.6770833333 |
| Leu | 3 | 10.9375 |
| Leu | 4 | 11.1979166667 |
| Ser | 5 | 9.63541666667 |
| Ser | 6 | 9.63541666667 |
| Ala | 7 | 8.85416666667 |
| Glu | 8 | 9.11458333333 |
| Ala | 9 | 8.07291666667 |
| Leu | 10 | 11.4583333333 |

Table 6: Most Frequent Residues in Non- Phosphorylated Group at Respective Positions between -10 to 10

| AA | -10 | -9 | -8 | -7 | -6 | -5 | -4 | -3 | -2 | -1 | 1 | 2 | 3 | 4 | 5 | 6 | 7 | 8 | 9 | 10 |
|---|---|---|---|---|---|---|---|---|---|---|---|---|---|---|---|---|---|---|---|---|
| Ala | | | | | | | | | | | | | | | | | F | | F | |
| Cyc | | | | | | | | | | | | | | | | | | | | |
| Asp | | | | | | | | | | | | | | | | | | | | |
| Glu | | | F | | | F | | | | | | F | | | | | | F | | |
| Phe | | ■ | | | | | ■ | | | | | | | | | | | | | |
| Gly | | | | | | | | | | | | | | | | | | | | |
| His | | | | | | | | ■ | X | | | | | | | | | | | |
| Ile | | | | ■ | | | | | | | | ■ | | | | | | | | |
| Lys | | | | | | | | ■ | | | | | | | | | | | | |
| Leu | F | F | | F | F | | F | F | | F | | | F | F | | | | | | F |
| Met | | | | | | | | | | | | | | | | | | | | |
| Asn | | | | | | | | | | | | | | | | | | | | |
| Pro | | | | | | | | | | | | | | | | | | | | |
| Gln | | | | | | | | | | | | | | | | | | ■ | | |
| Arg | | | | | | | | | | | | | | | ■ | | | | | |
| Ser | | | | | | | | | F | | F | | | | F | F | | | | |
| Thr | | | | | | | | | | | | | | | | | | | | |
| Val | | | | | | | | | | | | | | | | | | | | |
| Trp | | | | X | | | | X | | ■ | | | | | | | | | | |
| Tyr | | ■ | | | | | | | | | | | | | | | | | | |

| | |
|---|---|
| X | Represents those Sites where the corresponding Amino Acid at the corresponding Position is absent |
| F | Represents those Sites where the corresponding Amino Acid at the corresponding Position is Most Frequent |
| ■ | Represents those Sites where the corresponding Amino Acid at the corresponding Position is Significantly Preferred |

Table7: Non-Phosphorylated Group

## 4. CONCLUSION

This study performs statistical analysis to estimate preference of amino acids in the vicinity of EGFR Kinase based phosphorylated Tyr and non-phosphorylated Tyr. This study suggests that Gly at -6, Glu at -3 and Val at +1 play an important role in the phosphorylation of Tyr with EGFR Kinase. Moreover, Ala, Cys, Phe, Gly. His. Ile. Lys. Leu. Met. Asn. Gln. Arg. Ser. Thr. Trp. Tyr may also play an important role as they have been found to be absent in the vicinity at various positions. On the other hand, Phe, Tyr, Ile, Lys, His, Trp, Arg and Gln were found to be statistically preferred in the vicinity of non-phosphorylated Tyr. Furthermore, this study suggests that His at position -2 and Trp at positions -7 and -3 may have important role in non-phosphorylation activities.

## REFERENCES

1. P.Bork, T.Dansekar, Y. Diaz-Lazcoz, F. Eisenhaber, M.Huynen, and Y. Yuan, Predicting function: from genes to genome and back. J. Mol. Biol, 283, 707-725. (1998)
2. T.Attwood, Int. J. Biochem. Cell Biol, 32, 139-155. (2000)
3. T.H.T. Christlet and K. Veluraja, Biophys.J., 80,952-960. (2001)
4. W.M.Qazi, M. Ahmed, D.C. Hoessli, I.Ahmad, I.Khawaja, T.Wajahat, A.Kaleem, E. Walker-Nasir, N. Rehman, A.R. Shakoori and Nasir-ud-Din.. Pakistan J. Zool. 38, 55-63 (2006).
5. K.S.Kolibaba and B.J Kruker, Biochim.biophys.Acta., 1333 F217-F248 (1997)
6. T. Hunter, Philos.Trans.R.Soc.Lond.B Biol.Sci.,353, 583-605(1998)
7. Z, Songyang, S, Blechner, N, Hoagland, M.F. Hoekstra, H. Piwnica-Worms and L.C. Cantley, Curr.Biol., 4, 973-982 (1994)
8. F.Diella, F.Cameron, C.Gemund, R.Linding, A.Via, B.Kuster, T,Sicheritz-Ponten, N.Blom and T.Gibson, BMC Bioinform., 5, 79(2004)
9. W.M.Qazi, Bioinformatics: Analysis of Phospho-proteins Using Machine Learning Methodology. M.Phil Thesis, School of Computer Sciences, National College of Business Administration and Economics (2007)